Article

Dynamic Modeling of a HeXe-Cooled Mobile Nuclear Reactor with Closed Brayton Cycle

Jiaolong Deng [1,2]**, Chaoran Guan** [1,2]**, Xiaojing Liu** [1,2] **and Xiang Chai** [1,2,*]

1   School of Mechanical Engineering, Shanghai Jiao Tong University, 800 Dongchuan Road,
    Shanghai 200240, China; aspiration@sjtu.edu.cn (J.D.); guanchaoran@sjtu.edu.cn (C.G.);
    xiaojingliu@sjtu.edu.cn (X.L.)
2   Shanghai Digital Nuclear Reactor Technology Integration Innovation Center, Shanghai 200240, China
*   Correspondence: xiangchai@sjtu.edu.cn

Abstract: Helium-xenon (HeXe)-cooled mobile nuclear reactors have promising potential in future low-carbon energy systems. However, there is currently a lack of fast and reliable tools for analyzing the complicated dynamic characteristics of such systems. In this study, we developed a comprehensive dynamic modeling approach for a HeXe-cooled nuclear power system coupled with a closed Brayton cycle (CBC). The system's key components, including the reactor, printed circuit heat exchanger (PCHE), and turbomachinery, are lumped-modeled to capture their time-varying behavior. A step-solving algorithm that incorporates HeXe mass conservation iteration is designed. The verification results demonstrate that the dynamic program is robust and reliable, with each time step converging within 25 iterations and the HeXe mass remaining within the range of 3.755 ± 0.01 kg throughout the simulation meeting the law of mass conservation. Then, a 1500 s frozen start-up simulation for the coupled system is conducted, in which the CBC is started in the first 500 s by increasing the main shaft speed to 40% of the rated value, and then the reactor is started by inserting external reactivity between 500 and 800 s. Both the dynamic process and the steady-state performance after the start-up are analyzed. The results show that the system achieved a stable electrical output of 5.7 MWe with a thermal efficiency of 32.5%. This study lays a solid foundation for future work aimed at improving the overall efficiency and performance of HeXe-cooled nuclear power systems.

Keywords: HeXe mixture; closed Brayton cycle; solid nuclear reactor; lumped modeling; mass conservation

1. Introduction

In recent years, advanced small mobile nuclear reactors gained attention due to their flexibility when deployed in remote areas. These reactors provide a reliable source of energy that can be quickly installed, making them valuable for regions where conventional power grids are not feasible [1]. Their potential to enhance future energy systems aligns with global efforts toward green, low-carbon, and sustainable development. Among these technologies, the helium-xenon (HeXe)-cooled solid-state nuclear reactor stands out as a promising candidate for a mobile nuclear power source [2]. The HeXe mixture, used as a coolant in the reactor core, offers excellent thermal properties and compressibility, which are critical for maintaining efficient heat transfer [3]. Furthermore, this reactor operates based on an advanced closed Brayton cycle (CBC), known for its high thermal efficiency. As a result, the HeXe-cooled solid-state reactor represents a forward-looking technological route with significant potential for both energy security and environmental sustainability in the future.

Currently, numerous investigations can be found on sCO_2-cooled nuclear reactor systems coupled with CBC [4–6], while those on HeXe-cooled power systems are still limited and thus need to be further focused on. Over the years, some conceptual designs for HeXe-cooled reactors were preliminarily proposed, particularly for space and mobile

power systems. The Prometheus project of the United States was proposed in the 2000s [7], which introduced a 1 MWt HeXe-cooled reactor designed for space propulsion and long-term energy supply. This design featured 288 UO_2 fuel rods arranged compactly with a combination of sliding reflector segments and a central emergency rod to minimize weight and volume. In 2009, Gallo [8] proposed a Brayton rotating unit system for space reactor power, using a HeXe mixture in a CBC. Their design achieved up to 26% thermal efficiency, making it a promising candidate for high-efficiency space reactors. More recently, Meng [9] conducted a neutronics analysis of a megawatt-class HeXe-cooled reactor, focusing on the use of annular UO_2 fuel rods and various control rod configurations to optimize reactivity and neutron management. Guan [10] then proposed a micro-transportable gas-cooled reactor using a HeXe mixture, with core mass optimization achieved through BeO moderators and reflector sliders, offering a portable and long-term power solution. In addition, Ma [11] explored the load loss characteristics of space nuclear power systems, emphasizing the role of multiple Brayton loops in maintaining system safety and performance during power fluctuations. These designs collectively mark significant advancements in HeXe reactor technologies for space and mobile applications.

Despite the significant progress in developing steady-state conceptual designs, there remains a pressing need to focus on optimizing design parameters for the system dynamic behavior. The complexity of the HeXe-cooled reactor system lies not only in its individual components, such as the reactor core, printed circuit heat exchanger (PCHE), and turbomachinery, but also in the intricate coupling and dynamic interactions between these elements. The behavior of each component influences the overall system's response under varying operational conditions.

Numerous methods were used to analyze the dynamic performance of HeXe-cooled nuclear reactor-powered systems. On the experimental side, Wright [12] conducted operational tests on a CBC test-loop at Sandia National Laboratories (SNL). The test loop was designed to simulate the operational behavior of reactor-driven CBC systems using HeXe gas mixtures, proving the feasibility of such a novel power system, and providing valuable data for validating their system models. Despite the insights gained from these experiments, challenges such as high costs, long testing periods, and limited data acquisition restrict their widespread use.

Consequently, researchers increasingly turned to simulation programs for analysis. Wang [13] developed a dynamic simulation code for gas-cooled reactors using a CBC system. Their simulation examined transient behaviors and operational conditions, demonstrating the system's inherent safety and reliability during reactivity insertion accidents. Meng [14] further enhanced simulation efforts by developing a one-dimensional simulation code SIMCODE for space nuclear reactors, focusing on transient accident conditions and system safety evaluations. Additionally, Wang [15] created a HeXe mixture physical property calculation program and validated it through comparisons with existing data, which proved highly accurate. Liao [16] developed a Brayton cycle system analysis program for a HeXe-cooled nuclear reactor, focusing on dynamic simulation of system operating characteristics under various reactivity control methods and analyzing the effects of altitude and flight speed on power and heat dissipation. These simulation efforts provide a cost-effective and efficient means of studying HeXe reactor designs, offering deeper insights into system behavior without the limitations of experimental testing.

Although various dynamic simulation programs have been developed, most are tailored to space applications [14,17], leaving a gap in the tools available for land-based, mobile nuclear power systems. The unique operational demands of mobile systems, especially under dynamic conditions, require more specialized tools. Therefore, there is an urgent need to develop simplified, fast lumped-parameter simulation models. Such tools would allow for more efficient evaluation of the operational characteristics of HeXe-cooled nuclear power systems under dynamic conditions, providing valuable insights for the optimization of system parameters and guiding the development of more robust designs.

This paper presents the development of a dynamic analysis program for a land-based HeXe-cooled mobile nuclear power system. The program focuses on capturing the transient thermohydraulic characteristics of those key individual components, including the reactor, PCHE, and turbomachinery, through lumped-parameter mathematical modeling. A core feature of the program is the incorporation of a closed-cycle mass conservation algorithm, enabling accurate dynamic simulations of the system's performance. The validity of the developed program was tested, demonstrating its capability to model real-world scenarios and achieve HeXe mass conservation of a closed-cycle system. Finally, a system startup condition is simulated, and the results show that the system successfully completes the startup process, achieving an overall thermal efficiency of 32.5%. This work provides a foundation for further optimization and analysis of mobile nuclear power systems operating under dynamic conditions, addressing a critical gap in current research and offering a valuable tool for future system designs.

2. Methodology

In this section, the layout and working principle of the nuclear-powered HeXe CBC is briefly introduced. Next, the detailed modeling of the key components as well as their mathematical expressions are given. Finally, the calculation flowchart of the system dynamic operation is explained, including the iteration of HeXe mass conservation in the closed cycle.

2.1. Introduction of the Power System

The gas-cooled nuclear reactor system operates based on a closed Brayton cycle, utilizing a HeXe gas mixture as the working fluid. As shown in Figure 1, the system consists of several key components, including the reactor core, a compressor, a turbine, a recuperator, and a precooler. The gas coolant absorbs heat from nuclear fission in the reactor. The heated gas (point 4) is directed into the turbine (point 5), where its thermal energy is converted into mechanical energy to generate electricity. After passing through the turbine, the gas enters the recuperator (point 3). In fact, the recuperator plays a critical role in improving overall cycle efficiency by recovering residual heat from the working fluid before it is cooled further in the next step. The extracted heat is reused to preheat the incoming cooler gas that will enter the reactor, thus reducing the energy needed to reheat it in the reactor. Next, the cooled gas moves to the precooler (point 6), where external air (point 7 and 8) is used to reduce its temperature further. The gas is subsequently compressed in the compressor (point 2) to raise its pressure, preparing it for re-entry into the reactor core to repeat the cycle.
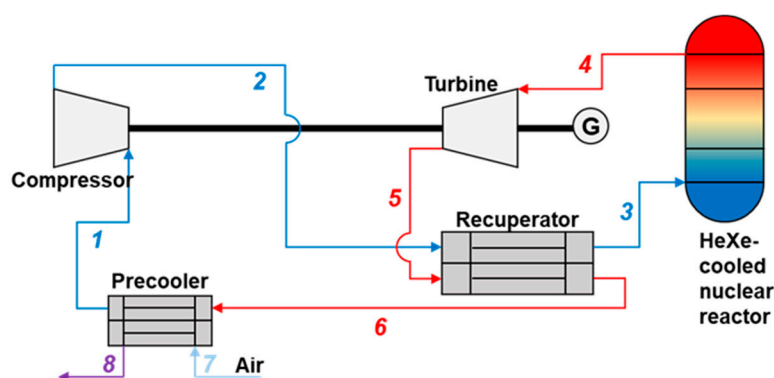

Figure 1. Schematic diagram of the HeXe closed Brayton cycle.

This closed-loop system is highly efficient, as it continually recycles the HeXe mixture, minimizing losses and optimizing the conversion of thermal energy into electrical energy. The use of helium and xenon as the working fluid is particularly advantageous due to their

excellent thermodynamic properties, such as high thermal conductivity and low neutron absorption cross-section, making the system suitable for mobile nuclear power generation.

2.2. Turbomachine Modeling

The turbomachinery consists of a compressor, a turbine, and an alternator, and they play critical roles in the CBC power system. The performance of these components is characterized by their pressure and temperature ratios. As described in Equation (1), the pressure ratio (π) and temperature ratio (σ) for both the compressor and turbine are functions of the HeXe mass flow rate ($\dot{m}$) and the shaft rotational speed (N). For the compressor, subscripts 1 and 2 are at its inlet and outlet, respectively. Similarly, subscripts 4 and 5 are the turbine inlet and outlet, respectively.

$$
\begin{aligned}
\pi_{comp} &= \frac{P_2}{P_1} = f_{\pi,c}(\dot{m}, N) \\
\sigma_{comp} &= \frac{T_2}{T_1} = f_{\sigma,c}(\dot{m}, N) \\
\pi_{tur} &= \frac{P_4}{P_5} = f_{\pi,t}(\dot{m}, N) \\
\sigma_{tur} &= \frac{T_4}{T_5} = f_{\sigma,t}(\dot{m}, N)
\end{aligned}
\tag{1}
$$

The performance curves illustrate the relationships between the mass flow rate, rotational speed, and the pressure and temperature ratios for both the compressor and turbine under off-design operating conditions. These curves are essential for understanding the dynamic response of the CBC power system. The performance curve shown in Figure 2 originates from those of a 132 kWe turbomachine designed by the Prometheus project [17], with a similar variation tendency, but the values are scaled based on our own design.
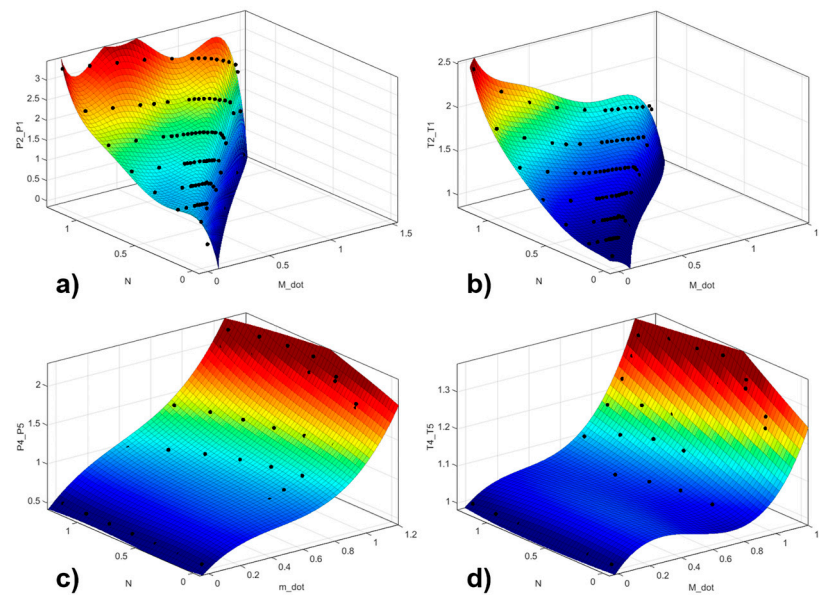

Figure 2. Performance curve of the turbomachine: (**a**) compressor pressure ratio; (**b**) compressor temperature ratio; (**c**) turbine pressure ratio; and (**d**) turbine temperature ratio.

Equation (2) outlines the work accomplished by the compressor and turbine, which are the functions of the mass flow rate and the enthalpy difference across the components. The network output of the system is the difference between the turbine's work and the compressor's work.

$$
\begin{aligned}
W_c &= \dot{m} C p_{12}(T_2 - T_1) \\
W_t &= \dot{m} C p_{45}(T_4 - T_5) \\
W_{net} &= W_t - W_c
\end{aligned}
\tag{2}
$$

2.3. Reactor Thermal Modeling

The point kinetic (PK) model is used to describe the time-varying features of the reactor. This simplified model states that the spatial shapes of the angular flux and the precursor concentrations remain in the fundamental mode during the transient period, while only the amplitudes change. It consists of seven ordinary differential equations (ODEs), resulting in a fast solution in dynamic neutronics analysis for the nuclear-powered system:

$$
\begin{aligned}
\frac{dQ_{core}}{dt} &= \frac{\rho - \beta}{\Lambda} Q_{core} + \sum_{i=1}^{6} \lambda_i C_i \\
\frac{dC_i}{dt} &= \frac{\beta_i}{\Lambda} Q_{core} - \lambda_i C_i \\
\rho &= \rho_e + \rho_d \\
\Delta \rho_f &= -f(\Delta T_{core})
\end{aligned}
\tag{3}
$$

where Q_{core} is the nuclear power and ρ is the reactivity. Λ, β_i, λ_i, and C_i represent the point kinetic parameters, whose values are obtained by the pre-conducted Monte Carlo modeling of the reactor [10]. The net reactivity is divided into external reactivity ρ_e and feedback reactivity ρ_d. Temperature feedback can significantly influence the safety of a nuclear system, and its specific form can be found in our previous study [18].

Figure 3 shows the structure of 1/12 of the solid-state gas-cooled reactor core, which is composed of multiple hexagonal units. Each contains key components such as the fuel, cladding, HeXe coolant, and the matrix material. The yellow regions represent the fuel, the black areas denote the matrix, the blue represents the HeXe mixture used for cooling, and the beige indicates the cladding material, which encapsulates the coolant channel.
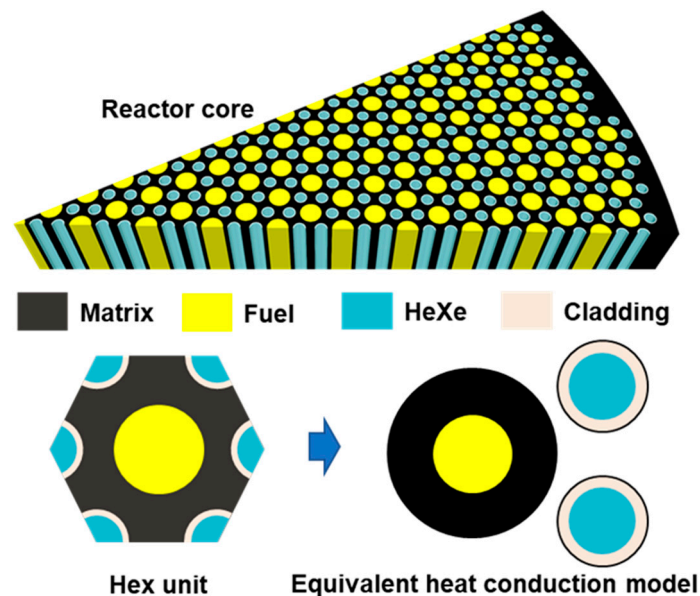

Figure 3. Structure and modeling of the nuclear reactor core.

To simplify the heat conduction calculations, the hexagonal unit is simplified into an equivalent cylindrical heat conduction model based on the principle of the equivalent area. In fact, the equivalent area method is commonly used to simplify and analyze heat transfer behaviors of the irregular geometry of the cylindrical solid-state reactor core [19]. This transformation enables easier computation of heat transfer through the reactor core by modeling the system as concentric cylindrical layers. The fuel is represented by the innermost circle, surrounded by layers representing the cladding, HeXe coolant, and matrix. The heat conduction from the fuel to the coolant and ultimately to the matrix can then be analyzed as a radial heat flow.

The fuel temperature can be solved by the following equation:

$$m_{fuel}Cp_{fuel}\frac{dT_{fuel}}{dt} = Q_{core} - \frac{\left(T_{fuel}-T_{mono}\right)}{Res_{fuel-mono}}$$

$$Res_{fuel-mono} = \frac{1}{4\pi L_{core}\kappa_{fuel}} + \frac{ln\left(\frac{\frac{r_{fuel}+r_{mono}}{2}}{r_{fuel}}\right)}{2\pi L_{core}\kappa_{mono}} \tag{4}$$

The matrix temperature can be solved by the following equation:

$$m_{mono}Cp_{mono}\frac{dT_{mono}}{dt} = \frac{\left(T_{fuel}-T_{mono}\right)}{Res_{fuel-mono}} - \frac{\left(T_{mono}-T_{clad}\right)}{Res_{mono-clad}}$$

$$Res_{mono-clad} = \frac{ln\left(\frac{r_{mono}}{\frac{r_{fuel}+r_{mono}}{2}}\right)}{2\pi L_{core}\kappa_{mono}} + \frac{ln\left(\frac{\frac{r_{ci}+r_{cs}}{2}}{r_{cs}}\right)}{4\pi L_{core}\kappa_{clad}} \tag{5}$$

where r_{cs} and r_{ci} are the outer and inner radius of the small cladding ring. The cladding temperature can be solved by the following equation:

$$m_{clad}Cp_{clad}\frac{dT_{clad}}{dt} = \frac{\left(T_{mono}-T_{clad}\right)}{Res_{mono-clad}} - \frac{\left(T_{clad}-T_{34}\right)}{Res_{clad-flow}}$$

$$Res_{clad-flow} = \frac{ln\left(\frac{r_{ci}}{\frac{r_{ci}+r_{cs}}{2}}\right)}{4\pi L_{core}\kappa_{clad}} + \frac{1}{4\pi r_{ci}L_{core}h} \tag{6}$$

where h is the heat transfer coefficient of the HeXe coolant flowing through the channel, and the Nu number can be evaluated by the Dittus–Boelter equation [20]:

$$Nu = 0.023Re^{0.8}Pr^{0.4}. \tag{7}$$

At the reactor outlet, the HeXe temperature can be calculated by the law of energy conservation:

$$Cp_{34}\frac{dm_{34}T_4}{dt} = \frac{\left(T_{clad} - T_{34}\right)}{Res_{clad-flow}} - \dot{m}Cp_{34}(T_4 - T_3). \tag{8}$$

2.4. PCHE Thermal Modeling

The PCHE is commonly used as the heat exchanger in the CBC, since it features compactness, high reliability, and effectiveness under extreme working conditions [21]. In our past study on the conceptual design of the whole CBC system configuration, the finned tube cross-flow heat exchanger and the PCHE were evaluated and discussed, indicating that the PCHE has a smaller footprint and thus is more appropriate to meet the compactness requirement of the mobile power system [22]. The PCHE shown in Figure 4 consists of alternating semicircular hot and cold channels embedded in a solid block. Hot fluid flows through the red channels, while cold fluid flows through the adjacent blue channels in a counter-flow arrangement. This setup maximizes the temperature gradient between the fluids, ensuring efficient heat transfer. The key parameters, such as channel diameter, pitch, and thickness, optimize heat exchange while maintaining a compact design. This efficient thermal management is crucial for maintaining the system's overall performance.
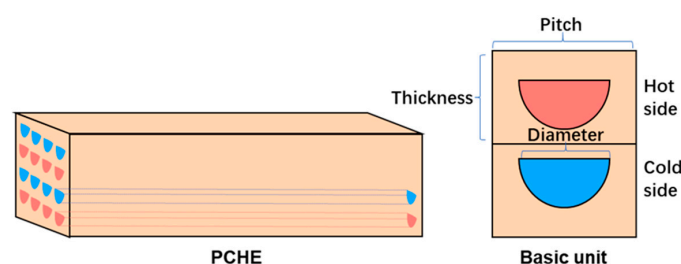

Figure 4. Schematic diagram and modeling of the PCHE.

For the recuperator, the cold side outlet temperature T_3, the solid structure temperature T_{rcp}, and the hot side outlet temperature T_6 can be solved by the following equations, respectively:

$$Cp_{23}\frac{dm_{23}T_3}{dt} = U_{23}A_{23}(T_{rcp} - T_{23}) - \dot{m}Cp_{23}(T_3 - T_2) \tag{9}$$

$$m_{rcp}Cp_{rcp}\frac{dT_{rcp}}{dt} = U_{56}A_{56}(T_{56} - T_{rcp}) - U_{23}A_{23}(T_{rcp} - T_{23}) \tag{10}$$

$$Cp_{56}\frac{dm_{56}T_6}{dt} = U_{56}A_{56}(T_{rcp} - T_{56}) - \dot{m}Cp_{56}(T_6 - T_5). \tag{11}$$

For the precooler, the cold side outlet temperature T_1, the solid structure temperature T_{prc}, and the hot side outlet temperature T_6 can be solved by the following equations, respectively:

$$Cp_{61}\frac{dm_{61}T_1}{dt} = U_{61}A_{61}(T_{pcc} - T_{61}) - \dot{m}Cp_{61}(T_1 - T_6) \tag{12}$$

$$m_{prc}Cp_{prc}\frac{dT_{prc}}{dt} = U_{61}A_{61}(T_{61} - T_{prc}) - U_{78}A_{78}(T_{prc} - T_{78}) \tag{13}$$

$$m_{78}Cp_{78}\frac{dT_8}{dt} = U_{78}A_{78}(T_{prc} - T_{78}) - \dot{m}_{78}Cp_{78}(T_8 - T_7) \tag{14}$$

where T_7 is the inlet temperature of the second side of the precooler, with a fixed value of 300 K.

In the above equations, U and A mean the equivalent heat transfer coefficient and heat transfer area of the PCHE channels. For instance, those parameters of the recuperator cold side with semicircle channels can be evaluated by the following equations [4]:

$$\frac{1}{U_{23}} = \frac{1}{h_{23}} + \frac{\vartheta_{eqn}}{2\kappa_{struc}}$$
$$\vartheta_{eqn} = \vartheta - \pi\frac{d_{channel}}{8} \tag{15}$$
$$A_{23} = N_{rcp,cold}L_{reg}\left(\frac{\pi}{2} + 1\right)d_{channel}$$

where h_{23} is the convection heat transfer coefficient, which can also be evaluated by the D-B equation shown in Equation (7), ϑ_{eqn} is the equivalent plate thickness, and $N_{rcp,cold}$ is the channel number of the recuperator cold side.

2.5. HeXe Pressure and Mass Calculation

The pressure drop when the HeXe mixture flows through the reactor, the recuperator, and the precooler can be evaluated based on Darcy's law:

$$P_{out} = P_{in} - \frac{fL\dot{m}^2}{2\rho A^2 d_h} \tag{16}$$

where d_h is the hydraulic diameter of the channel, and f is the friction factor, which can be calculated by empirical correlations based on the flow Re number, as shown in Figure 5. Specifically, when the gas mixture flows at the transition region, a smooth linear interpolation of f is used to avoid possible divergence in the mass conservation iteration when conducting dynamic simulation.

For the closed cycle, the pressure values of different locations of the CBC can be determined if the pressure drop across components and the pressure ratio of the turbomachine have been obtained:

$$(P_1\pi_c - \Delta P_{23} - \Delta P_{34})/\pi_t - \Delta P_{56} - \Delta P_{61} = P_1. \tag{17}$$
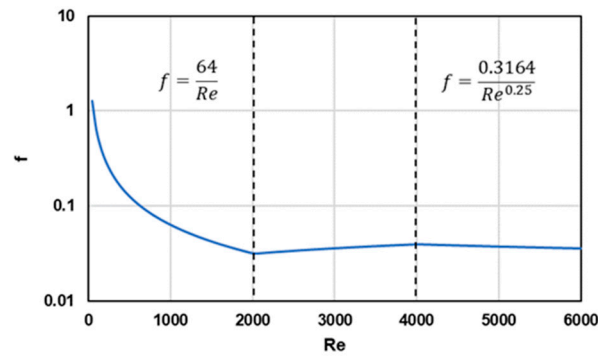
Figure 5. Friction factor as the function of *Re* number.

The total HeXe mass of the closed cycle can be calculated based on the state equations after the temperature and pressure of the gas mixture in different locations have been obtained:

$$m_{hexe} = m_{61} + m_{23} + m_{34} + m_{56} = \sum \frac{P_i V_i}{R_g T_i} \tag{18}$$

where R_g is the gas constant of the HeXe mixture.

In addition, thermal properties of the solid materials are set as fixed values. Density of the air and the HeXe mixture will be updated based on state equations, and other thermal properties of the gas are also set as constants. For the HeXe mixture with the Xenon fraction of 12%, the specific heat, the thermal conductivity, and the dynamic viscosity are set as 1079 J/kg-K, 0.2471 W/m-K, and 5.91×10^{-5} Pa-s.

2.6. Dynamic Simulation Process

Table 1 lists the key unknown parameters of the nuclear-powered HeXe CBC and their corresponding equations, based on the modeling framework presented in the above contents. These equations are combined and can be treated by the Python ODE solvers. Therefore, the reactor core nuclear power as well as the temperature distributions of the CBC can be determined in dynamic simulations.

Table 1. Unknowns to be solved by ODEs.

No.	Unknown Parameter	Corresponding ODE
1	T_{fuel}	Equation (4)
2	T_{mono}	Equation (5)
3	T_{clad}	Equation (6)
4	T_4	Equation (8)
5	T_3	Equation (9)
6	T_{rcp}	Equation (10)
7	T_6	Equation (11)
8	T_1	Equation (12)
9	T_{prc}	Equation (13)
10	T_8	Equation (14)
11	Q_{core}	Equation (1)
12~17	C_i	Equation (1)

The dynamic simulation process is shown in Figure 6. At each time step, the properties of the HeXe mixture are updated, followed by recalculating the turbomachinery working conditions. The PKEs and thermal ODEs are then solved to assess the reactor's nuclear and thermal behavior. Next, the pressure and mass equations are solved to maintain system balance. A key step in the process is checking whether the HeXe flow rate satisfies the mass conservation criterion:

$$\left| m_{hexe} - m_{hexe,0} \right| < \varepsilon \tag{19}$$

where $m_{hexe,0}$ is the initial HeXe mass inside the cycle, and ε is the tolerance which controls the convergence of the iteration. If the criterion is not met, the flow rate is updated, and the simulation loop returns to adjust the turbomachinery state accordingly. This iterative process continues until mass conservation is achieved, advancing to the next time step.
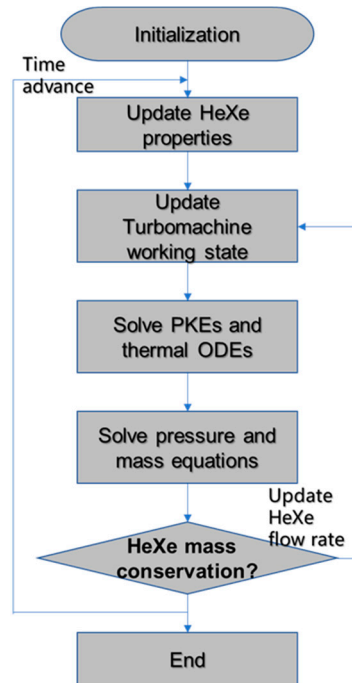

Figure 6. Dynamic simulation flowchart having HeXe mass conservation iteration.

3. Result and Discussion

The developed programs are used to simulate the dynamic operating processes of the nuclear-powered HeXe CBC system. In this paper, a start-up process lasting 1500 s is chosen as the classical case. Firstly, parameter settings are given. Next, variation in the HeXe mass during the simulation is presented to prove the correctness and reliability of the program. Then, involution of the key thermohydraulic parameters of the system during start-up is demonstrated and analyzed.

3.1. Case Setting

The geometric parameters of the power system components are outlined in Table 2. The reactor core has a length of 1 m, with key dimensions including a core radius of 0.44 m and a fuel-to-coolant pitch of 15 mm. The cladding thickness is set at 0.5 mm to ensure thermal and structural integrity. For the heat exchangers, both the recuperator and precooler are modeled as PCHE. The recuperator has a channel diameter of 1.5 mm and consists of 480 channels per layer, with a total of 1346 layers. The precooler has a channel diameter of 3 mm, with 361 channels per layer and 880 layers overall. These configurations are designed to optimize heat transfer efficiency and compactness, which is essential for a high-performance system.

For the start-up simulation, the initial conditions are listed in Table 3. The reactor begins with an initial thermal power of 20 kWt, approximately 1/1000 of its rated power, to ensure a controlled start. The initial shaft speed is set to 1/100 of the rated value. The initial HeXe flow rate is set to 1/100 of the rated value, corresponding to 0.6 kg/s, and the air flow rate is similarly reduced to 1/100 of its rated 70 kg/s. The system starts at an initial temperature of 300 K, simulating ambient conditions before the reactor heats up. Additionally, the initial HeXe pressure is set at 0.7 MPa to match expected operational conditions. These conservative settings are chosen to allow for a gradual ramp-up of the

system, ensuring safe and stable operation as the simulation progresses toward full power. This approach helps analyze the system's response to start-up transients and its ability to reach a steady operational state. The total start-up simulation time is expected to be within 1500 s under the single time step of 0.5 s. Particularly, a tolerance ε with the value of 0.01 kg is set to control the accuracy of the mass calculation, and the maximum mass conservation iteration per time step is set to 50 to avoid program freezes.

Table 2. Geometrical dimensions for key components of the power system.

Components	Parameters
Reactor	Length: 1 m
	Core radius: 0.44 m
	Fuel radius: 7.5 mm
	coolant channel radius: 4 mm
	Fuel-to-coolant pitch: 15 mm
	Cladding thickness: 0.5 mm
Recuperator (PCHE)	Length: 0.738 m
	Channel diameter: 1.5 mm
	Channel pitch: 2.1 mm
	Channel thickness: 1.45 mm
	Channel numbers per layer: 480
	Layer numbers: 1346
Precooler (PCHE)	Length: 0.3 m
	Channel diameter: 3 mm
	Channel pitch: 3.6 mm
	Channel thickness: 3.17 mm
	Channel numbers per layer: 361
	Layer numbers: 880

Table 3. Initial conditions for start-up simulation.

Parameters	Value
Initial reactor thermal power	20 kWt
Initial shaft rotational speed	1/100 of the rated value
Initial HeXe flow rate	1/100 of the rated 60 kg/s
Initial air flow rate	1/100 of the rated 70 kg/s
Initial system temperature	300 K
Initial HeXe pressure	0.7 MPa
Time step/Simulation time	0.5 s/1500 s
Mass conservation tolerance	0.01 kg
Maximum mass conservation iteration per time step	50

3.2. Code Verification

For code verification, the simulation results for the HeXe mass and the number of iterations required to maintain mass conservation over time are shown in Figure 7. During the start-up process, the number of iterations per time step varies with a maximum of 25, which is greatly below the set limit of 50 iterations. The HeXe mass remains within the range of 3.755 ± 0.01 kg, meeting the tolerance level of 0.01 kg set for the simulation. This indicates that the mass conservation condition was consistently satisfied throughout the simulation, ensuring that each time step in the dynamic analysis converged successfully. Moreover, the decreasing number of iterations required as the simulation progresses further highlights the program's efficiency in reaching mass conservation quickly as the system approaches steady-state conditions.
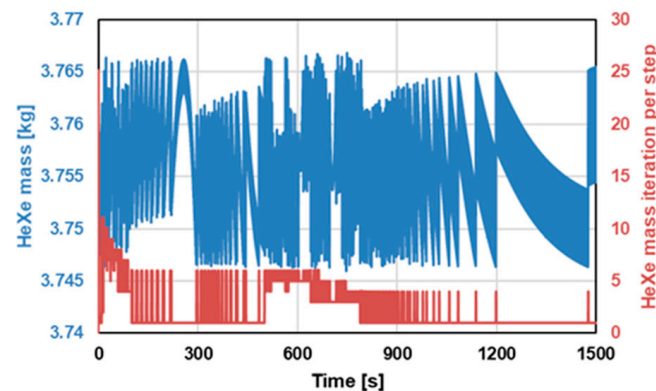
Figure 7. Code verification by checking HeXe mass conservation.

The verification results provide strong evidence for the reliability and accuracy of the developed dynamic simulation program. By successfully maintaining mass conservation under dynamic conditions, the program proves its robustness in handling the complexities of a HeXe-cooled reactor system. This ensures confidence in its ability to perform accurate simulations even during rapid changes in operational conditions, such as system start-up, shutdown, and other typical but complicated cases.

3.3. Start-Up Analysis

Figure 8 presents the simulation results of the system start-up process, demonstrating the evolution of key parameters over time. This process can be divided into three distinct phases: Phase 1 (0–500 s), Phase 2 (500–800 s), and Phase 3 (800–1500 s), each representing a critical stage in the system's gradual transition to full operation. These subplots track parameters such as mass flow rate, shaft speed, pressure ratios, reactivity, power output, and HeXe temperatures throughout the start-up. These graphs provide insights into how the system components, such as the turbomachinery, compressor, and reactor, interact dynamically during the start-up process. Additionally, plot (h) illustrates the steady-state temperature and pressure distributions across key points in the system once the start-up phase is complete. This figure highlights the operational states of the CBC at full power, offering a comprehensive view of how the system achieves equilibrium.

Overall, the start-up strategy can be concluded as starting the CBC first at the first 500 s, followed by starting the nuclear reactor by inserting some external reactivity at 500–800 s.

In Phase 1 (0–500 s), the system begins its initial start-up. Within the first 100 s, both the shaft speed N and the air mass flow rate $\dot{m}_{air}$ rapidly increase to approximately 40% of their rated values. According to the HeXe mass conservation results, the HeXe mass flow $\dot{m}_{hexe}$ stabilizes at around 26 kg/s. As shown by the characteristic curves, the compressor pressure ratio gradually increases and stabilizes at around 1.19. During this phase, the external reactivity ρ_e is kept at 0, and the reactor does not actively initiate fission reactions. Notably, despite the absence of nuclear heat generation, the HeXe mixture flows and expands through the turbine, causing the system's temperature to slightly drop by approximately 35 K [17]. Based on the temperature feedback effect, this temperature drop leads to a slight positive reactivity ρ_d, which in turn causes a passive and minor increase in nuclear reactor power output, reaching around 0.8 MWt. In terms of pressure, the HeXe loop pressure remains almost unchanged at approximately 0.7 MPa.
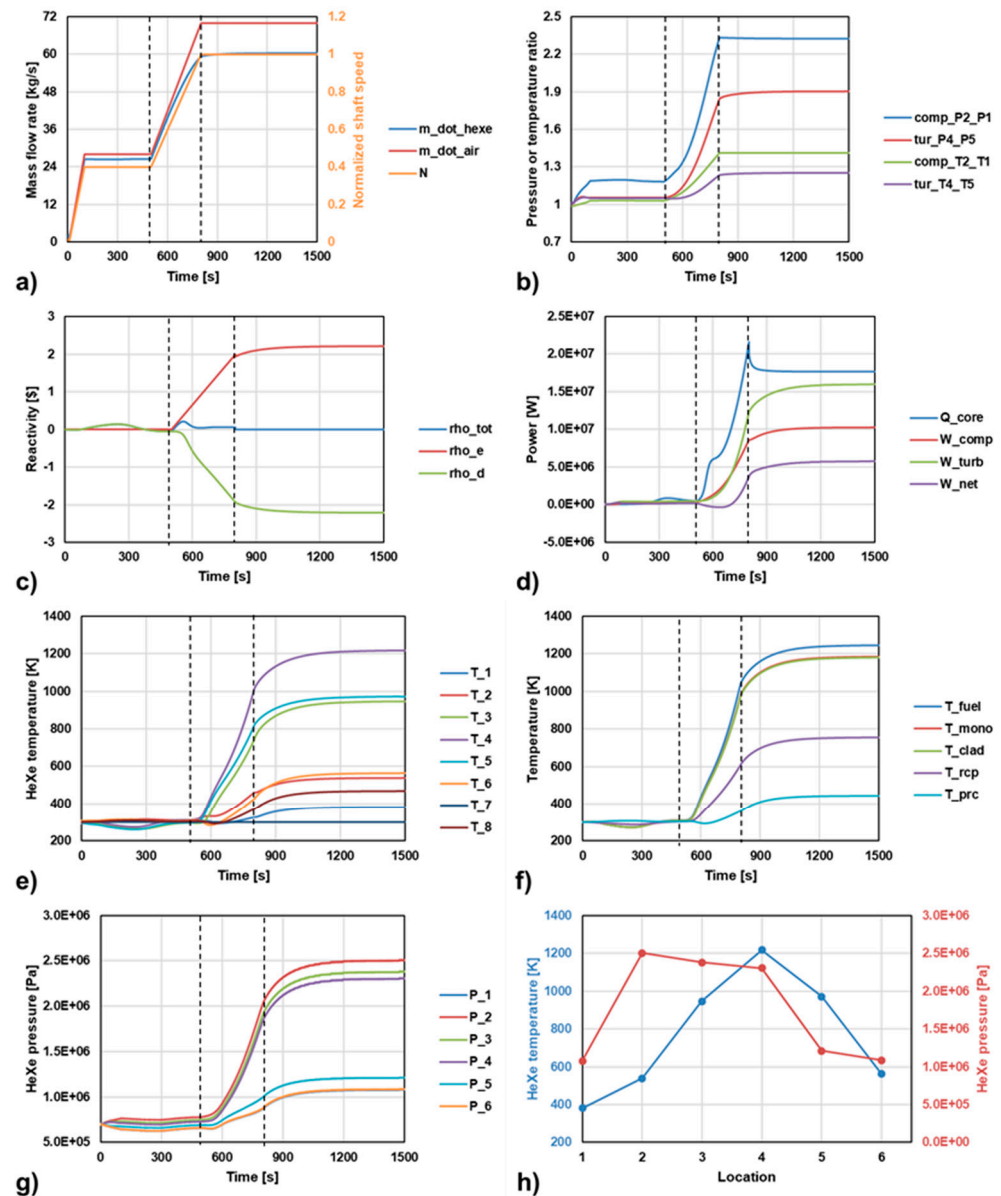
Figure 8. Simulation results of the system start-up in 1500 s. (**a**) Mass flow rate and shaft speed; (**b**) turbomachine working track; (**c**) reactivity; (**d**) power; (**e**) HeXe temperature of the CBC cycle; (**f**) solid component temperature; (**g**) HeXe pressure of the CBC cycle; and (**h**) HeXe temperature and pressure distributions when finishing start-up.

In Phase 2 (500–800 s), the external reactivity ρ_e is actively increased linearly from 0 to approximately USD 2. As a result, the power output and temperature of the solid-state reactor rise rapidly. With the reactor core temperature gradually reaching 1000 K, the negative reactivity ρ_d also increases gradually, and the total reactivity ρ_{tot} approaches zero. During this phase, the nuclear power output reaches approximately 20 MWt. To match the rising thermal output, both shaft speed N and the air mass flow rate $\dot{m}_{air}$ are increased from 40% to 100%. The HeXe mass flow $\dot{m}_{hexe}$ gradually rises to 60 kg/s, while the compressor pressure ratio increases to around 2.3, and the turbine pressure ratio rises to approximately 1.9. As shown in subplot (g), the pressure differential across the loop becomes evident, with a high pressure of around 2 MPa at the compressor outlet and a low pressure of about 1 MPa at the turbine inlet. Notably, from 500 to 700 s, the work consumed by the compressor is larger than that produced by the turbine, thus the system's net output

power W_{net} is negative. After 700 s, the system output power is positive and rises steadily, indicating that the system is transitioning smoothly toward full operation.

In Phase 3 (800–1500 s), the shaft speed N and the gas mass flow rates are maintained at 100%, while the external reactivity ρ_e is controlled to follow the variation in the temperature feedback reactivity ρ_d, causing the net reactivity ρ_{tot} to be equal to 0. The system's nuclear power output stabilizes at around 18 MWt, while the net output power of the CBC stabilizes at approximately 5.7 MWe, hence the overall thermal efficiency of the entire system reaches about 32.5%. The cycle effectiveness is determined by the design requirement of the mobile power system. The CBC effectiveness of the Prometheus project is 27% [17]. Hence, the calculated effectiveness by the dynamic start-up simulation in our system is reasonable. Subplot (h) shows the steady-state temperature and pressure distributions across the CBC loop. The whole loop can be clearly divided into high-pressure sections (point 2-3-4) and low-pressure sections (point 5-6-1). The maximum pressure is observed at the compressor outlet (point 2), reaching about 2.5 MPa, while the lowest pressure is at the turbine inlet (point 1), at approximately 1.07 MPa. The flow pressure loss across the nuclear reactor and the recuperator is larger than that across the precooler having a shorter length. The temperature differences between the reactor core and the recuperator are evident, with the highest temperature at the turbine outlet (point 4) reaching about 1200 K, and the lowest temperature at the compressor inlet (point 1) reaching around 400 K. The recuperator's internal temperature (between points 2 and 3) increases to about 407 K, significantly indicating the importance of the recuperator on enhancing the overall system efficiency. Notably, the temperature of the exhaust gas after passing through the secondary air cooler is still relatively high at 468 K, providing potential for further utilization, such as in an organic Rankine cycle (ORC) to improve overall system efficiency. With such energy recovery methods, the system's overall performance can be further optimized.

The conducted dynamic simulation results of the HeXe-cooled CBC system are compared with the published ones of the Prometheus project [17]. The design schemes of these two systems are quite similar by using the HeXe-cooled CBC configuration. In this MW-level land-based system, the low-enriched nuclear fuel and the graphite moderator is used for the reactor core, and the air-cooled pre-cooler is used as the heat sink. In the kW-level Prometheus space nuclear power system, the reactor is featured with a fast spectrum, and the radiation heat exchanger is used as the heat sink in the space environment. The mentioned differences about the system designs can lead to different point kinetic parameters and heat sink performance during the dynamic simulations. However, both the dynamic simulation codes are developed based on the lumped model and the law of mass and energy conservation. The overall tendencies of the start-up process and the evolution of cycle thermohydraulic parameters are similar.

4. Conclusions

This study presents a comprehensive dynamic modeling and analysis of a HeXe-cooled nuclear reactor coupled with a CBC power conversion system. The main findings and contributions can be summarized as follows:

1. Lumped-parameter mathematical models for the system's key components were developed, including the reactor, PCHE, and turbomachinery. These models describe the time-varying dynamic characteristics of each component, allowing for a detailed analysis of the system's performance under transient operating conditions.
2. A dynamic step-solving strategy based on the HeXe mass conservation iteration was designed. This approach ensures that the system remains accurate and stable throughout the simulation. Test results indicate that the number of iterations per time step did not exceed 25, and the converged transient HeXe mass remained consistently within the range of 3.755 ± 0.01 kg. These results demonstrate the reliability, robustness, and correctness of the dynamic program in meeting the law of HeXe mass conservation during the simulation.

3. A 1500 s frozen start-up analysis was conducted, simulating the system's start-up strategy of initiating the CBC first, followed by the reactor. The dynamic behavior of the system during start-up and its steady-state performance were thoroughly analyzed, focusing on critical issues such as temperature feedback effect and shaft speed matching principle. The results provide valuable insights into optimizing the system's efficiency and configuration. After finishing the start-up, the system achieved a stable electrical output of 5.7 MWe, with a thermal efficiency of approximately 32.5%. Although the system configuration and modeling parameters in this work are different from those in the Prometheus project, the overall start-up tendency is similar for the two systems.

These findings highlight the system's potential for further optimization in future designs.

Author Contributions: Conceptualization, J.D.; methodology, J.D.; software, J.D. and X.C.; validation, J.D. and C.G.; writing—original draft preparation, J.D.; writing—review and editing, X.L. and X.C. All authors have read and agreed to the published version of the manuscript.

Data Availability Statement: Data will be made available on request.

Conflicts of Interest: The authors declare no conflicts of interest.

References

1. Swartz, M.M.; Byers, W.A.; Lojek, J.; Blunt, R. Westinghouse eVinci™ Heat Pipe Micro Reactor Technology Development. *Am. Soc. Mech. Eng.* **2021**, *85246*, V001T04A018.
2. Hou, J.; Zhou, Y.; Huang, S. Conjugate Heat Transfer Analysis of Helium–Xenon Gas Mixture in Tight Rod Bundles. *Appl. Therm. Eng.* **2024**, *252*, 123661. [CrossRef]
3. Liu, Z.; Cheng, K.; Yin, Z.; Wang, Z.; Wang, J.; Qin, J. Evaluation of the CBC-ORC Energy System in Lunar Base: Working Fluid Combination Selection, Day and Night Operation Performance. *Energy Convers. Manag.* **2022**, *257*, 115445. [CrossRef]
4. Ming, Y.; Liu, K.; Zhao, F.; Fang, H.; Tan, S.; Tian, R. Dynamic Modeling and Validation of the 5 MW Small Modular Supercritical CO_2 Brayton-Cycle Reactor System. *Energy Convers. Manag.* **2022**, *253*, 115184. [CrossRef]
5. Sondelski, B.; Nellis, G. Mass Optimization of a Supercritical CO2 Brayton Cycle with a Direct Cooled Nuclear Reactor for Space Surface Power. *Appl. Therm. Eng.* **2019**, *163*, 114299. [CrossRef]
6. Wu, P.; Ma, Y.; Gao, C.; Liu, W.; Shan, J.; Huang, Y.; Wang, J.; Zhang, D.; Ran, X. A Review of Research and Development of Supercritical Carbon Dioxide Brayton Cycle Technology in Nuclear Engineering Applications. *Nucl. Eng. Des.* **2020**, *368*, 110767. [CrossRef]
7. Ning, K.; He, Y.; Huang, D.; Wang, X.; Yang, W.; Zhao, F.; Tan, S. Modelling Research on the Control Scheme and Control Characteristic of a Small Gas-Cooled Reactor. *Prog. Nucl. Energy* **2022**, *147*, 104189. [CrossRef]
8. Gallo, B.M.; El-Genk, M.S. Brayton Rotating Units for Space Reactor Power Systems. *Energy Convers. Manag.* **2009**, *50*, 2210–2232. [CrossRef]
9. Meng, T.; Zhao, F.; Cheng, K.; Zeng, C.; Tan, S. Neutronics Analysis of Megawatt-Class Gas-Cooled Space Nuclear Reactor Design. *J. Nucl. Sci. Technol.* **2019**, *56*, 1120–1129. [CrossRef]
10. Guan, C.; Chai, X.; Zhang, T.; Liu, X. Preliminary Lightweight Core Design Analysis of a Micro-Transportable Gas-Cooled Thermal Reactor. *Int. J. Energy Res.* **2022**, *46*, 17416–17428. [CrossRef]
11. Ma, W.; Ye, P.; Gao, Y.; Yang, X. Study on the Load Loss Characteristics of a Space Nuclear Power System with Multi Brayton Loops. *Ann. Nucl. Energy* **2023**, *185*, 109702. [CrossRef]
12. Wright, S.A. Dynamic Modeling and Control of Nuclear Reactors Coupled to Closed-Loop Brayton Cycle Systems Using SIMULINKTM. In Proceedings of the AIP Conference Proceedings; AIP: Albuquerque, NM, USA, 2005; Volume 746, pp. 991–1004.
13. Wang, C.; Zhang, R.; Guo, K.; Zhang, D.; Tian, W.; Qiu, S.; Su, G. Dynamic Simulation of a Space Gas-Cooled Reactor Power System with a Closed Brayton Cycle. *Front. Energy* **2021**, *15*, 916–929. [CrossRef]
14. Meng, T.; Cheng, K.; Zhao, F.; Xia, C.; Tan, S. Dynamic Simulation of the Gas-Cooled Space Nuclear Reactor System Using SIMCODE. *Ann. Nucl. Energy* **2021**, *159*, 108293. [CrossRef]
15. Wang, X.; Zhao, F.; He, Y.; Wang, X.; Tan, S.; Li, Z. Development and Verification of Helium–Xenon Mixture Cooled Small Reaction System. *Prog. Nucl. Energy* **2023**, *160*, 104679. [CrossRef]
16. Liao, H.; Zhao, F.; Ming, Y.; Cheng, K.; Wang, X.; Tan, S.; Tian, R. Precise Modelling and Operation Characteristics Analysis of the Small Helium-Xenon Gas Cooled Reactor Power System with the Air Heat Sink. *Ann. Nucl. Energy* **2024**, *204*, 110565. [CrossRef]

17. Wright, S.A.; Lipinski, R.J.; Vernon, M.E.; Sanchez, T. *Closed Brayton Cycle Power Conversion Systems for Nuclear Reactors*; Sandia National Lab. (SNL-NM): Albuquerque, NM, USA, 2006.
18. Deng, J.; Wang, T.; Liu, X.; Zhang, T.; He, H.; Chai, X. Experimental Study on Transient Heat Transfer Performance of High Temperature Heat Pipe under Temperature Feedback Heating Mode for Micro Nuclear Reactor Applications. *Appl. Therm. Eng.* **2023**, *230*, 120826. [CrossRef]
19. Labib, S.; King, J. Design and Analysis of a Single Stage to Orbit Nuclear Thermal Rocket Reactor Engine. *Nucl. Eng. Des.* **2015**, *287*, 36–47. [CrossRef]
20. Winterton, R.H. Where Did the Dittus and Boelter Equation Come From? *Int. J. Heat Mass Transf.* **1998**, *41*, 809–810. [CrossRef]
21. Olumayegun, O.; Wang, M.; Kelsall, G. Thermodynamic Analysis and Preliminary Design of Closed Brayton Cycle Using Nitrogen as Working Fluid and Coupled to Small Modular Sodium-Cooled Fast Reactor (SM-SFR). *Appl. Energy* **2017**, *191*, 436–453. [CrossRef]
22. Guan, C.; Chai, X.; Zhang, T.; Liu, X. Size Assessment of the Heat Exchanger for He-Xe Closed Brayton Cycle Applied in Mobile. In Proceedings of the Land-Based Microreactor System, Washington, DC, USA, 20 August 2023; pp. 3623–3636.